TEORIJSKA I PRIMENJENA MEHANIKA 20, pp 95–118, 1994, UDK 539.3

IMPLICIT STRESS INTEGRATION ALGORITHM FOR THE MODIFIED CAM–CLAY MATERIAL

M. Kojić, R. Slavković, N. Grujović, M. Vukićević

(Received 28.10.1994.)

Summary

An implicit computational algorithm for stress integration of the modified Cam-clay model is presented in the paper. The material behavior is described by ellipses with hardening characteristics, and with the critical stress state line.

The algorithm is developed for the strain-driven problems and it is employed in the incremental finite element analysis. The problem of stress calculation at the end of a load step is reduced to solution of one nonlinear equation, and the procedure represents an application of the governing parameter method (GPM) developed in Ref. [1]. Hardening and softening plasticity regimes are analyzed in detail. Derivation of the tangent constitutive elastic-plastic matrix, consistent with the stress integration algorithm, is also presented. This matrix provides the quadratic convergence rate in the incremental-iterative finite element analysis.

The algorithm is robust, reliable and efficient; and also it provides very good accuracy, illustrated through comparison with solutions available in cited references. It is especially suitable for the displacement based finite element analysis, and it has been implemented in the finite element general purpose program PAK.

Typical example of a real bearing capacity problem is solved, with application of the contact algorithm to model interaction between the structure and the soil.

1. Introduction

One of the key-steps in the inelastic finite element analysis [1] represents stress calculation, or stress integration, within the load (time) step. Significant efforts of researchers have been directed to the development of reliable, efficient and accurate stress integration algorithms [1], [3] to [10], [14], [15].

We present here a computational algorithm for stress integration of the modified Cam-clay material model. The algorithm represents an application

of the governing parameter method (GPM) developed in [1] for implicit stress integration of inelastic constitutive relations employed within incremental analysis of the strain-driven problems. We here outline shortly the basic concept of the GPM.

Let in an incremental solution procedure the known quantities be

$$ {}^{t}\underline{\sigma},\ {}^{t}\mathbf{e},\ {}^{t}\mathbf{e}^{IN},\ {}^{t}\underline{\beta},\ {}^{t+\Delta t}\mathbf{e} \tag{1} $$

and the unknowns at end of time step Δt are

$$ {}^{t+\Delta t}\underline{\sigma},\ {}^{t+\Delta t}\mathbf{e}^{IN},\ {}^{t+\delta t}\underline{\beta}, \tag{2} $$

where $\underline{\sigma}$, $\mathbf{e}$, $\mathbf{e}^{IN}$ and $\underline{\beta}$ are stresses, strains, inelastic strains and internal variables, respectively. The left superscripts "t" and "$t+\Delta t$" denote values at start and at end of time step. Then, the GPM consists in the following steps:

1. Express all unknowns in terms of one (governing parameter) p:

$$ \begin{aligned} {}^{t+\Delta t}\underline{\sigma} &= {}^{t+\Delta t}\underline{\sigma}\left({}^{t}\underline{\sigma},\ {}^{t}\mathbf{e},\ {}^{t}\mathbf{e}^{IN},\ {}^{t}\underline{\beta},\ {}^{t+\Delta t}\mathbf{e},\ p\right) \\ {}^{t+\Delta t}\mathbf{e}^{IN} &= {}^{t+\Delta t}\mathbf{e}^{IN}\left({}^{t}\underline{\sigma},\ {}^{t}\mathbf{e},\ {}^{t}\mathbf{e}^{IN},\ {}^{t}\underline{\beta},\ {}^{t+\Delta t}\mathbf{e},\ p\right) \\ {}^{t+\Delta t}\underline{\beta} &= {}^{t+\Delta t}\underline{\beta}\left({}^{t}\underline{\sigma},\ {}^{t}\mathbf{e},\ {}^{t}\mathbf{e}^{IN},\ {}^{t}\underline{\beta},\ {}^{t+\Delta t}\mathbf{e},\ p\right) \end{aligned} \tag{3} $$

2. Form a governing equation

$$ f(p) = 0 \tag{4} $$

and solve for ${}^{t+\Delta t}p$.

3. Substitute ${}^{t+\Delta t}p$ into (3) to obtain the unknowns quantities.

This computational procedure has been applied to various material models usually employed in engineering practice [1], [10], [16]–[20]. Also, it has been extended to viscoplasticity [21]. The most important features of the GPM are: the algorithm is robust, accurate (since it is implicit) and efficient (the problem is reduced to solution of one nonlinear equation (4)). We illustrate these characteristics in the Cam-clay model analyzed in the paper.

An important consequence of the approach outlined above is that it is possible to calculate, in a straightforward way, the true tangent constitutive matrix ${}^{t+\Delta t}\mathbf{C}$, as

$$ {}^{t+\Delta t}\mathbf{C} = \frac{\partial {}^{t+\Delta t}\underline{\sigma}}{\partial {}^{t+\Delta t}\mathbf{e}} = \frac{\partial {}^{t+\Delta t}\underline{\sigma}}{\partial {}^{t+\Delta t}p}\frac{\partial {}^{t+\Delta t}p}{\partial {}^{t+\Delta t}\mathbf{e}} \tag{5} $$

Derivatives $\partial {}^{t+\Delta t}p/\partial {}^{t+\Delta t}\mathbf{e}$ (with components $\partial {}^{t+\Delta t}p/\partial {}^{t+\Delta t}e_{ij}$) follows from differentiation of (4),

$$\frac{\partial f}{\partial^{t+\Delta t}\mathbf{e}} = \left(\frac{\partial f}{\partial^{t+\Delta t}\underline{\sigma}} \frac{\partial^{t+\Delta t}\underline{\sigma}}{\partial^{t+\Delta t}p} + \frac{\partial f}{\partial^{t+\Delta t}\mathbf{e}^{IN}} \frac{\partial^{t+\Delta t}\mathbf{e}^{IN}}{\partial^{t+\Delta t}p} + \right.$$
$$\left. + \frac{\partial f}{\partial^{t+\Delta t}\underline{\beta}} \frac{\partial^{t+\Delta t}\underline{\beta}}{\partial^{t+\Delta t}p} \right) \frac{\partial^{t+\Delta t}p}{\partial^{t+\Delta t}\mathbf{e}} + \frac{\partial f}{\partial^{t+\Delta t}\mathbf{e}} = 0 \quad (6)$$

For many material models in plasticity yield condition is defined in terms of the stress deviator $\mathbf{S}$, $\mathbf{S}=\underline{\sigma} - \underline{\sigma}_m$, where $\underline{\sigma}_m = \sigma_m \mathbf{I}$ is the mean stress and $\mathbf{I}$ is the identity tensor, i.e.

$$f_y = f_y(\mathbf{S}, \sigma_m) = 0 \quad (7)$$

We give here useful relations of the associative plasticity for the increments of plastic strains $\Delta\mathbf{e}^p$ in time step,

$$\Delta\mathbf{e}^p = \Delta\lambda \frac{\partial f_y}{\partial \underline{\sigma}} \quad (8)$$

where $\Delta\lambda$ is a positive scalar. From (7) and (8) follows:

$$\Delta\mathbf{e}^p = \frac{\Delta\lambda}{3} \left(\mathbf{D} \frac{\partial f_y}{\partial \mathbf{S}} + \frac{\partial f_y}{\partial \sigma_m} \right) \quad (9)$$

for normal components, and

$$\Delta\mathbf{e}^p = \Delta\lambda \frac{\partial f_y}{\partial \mathbf{S}} \quad (10)$$

for shear components, where

$$D = \begin{bmatrix} 2 & -1 & -1 \\ -1 & 2 & -1 \\ -1 & -1 & 2 \end{bmatrix} \quad (11)$$

is the coefficient matrix and $\partial f_y / \partial \mathbf{S}$ is a vector

$$\left(\frac{\partial f_y}{\partial \mathbf{S}} \right)^T = \left(\frac{\partial f_y}{\partial S_{11}}, \frac{\partial f_y}{\partial S_{22}}, \frac{\partial f_y}{\partial S_{33}}, \frac{\partial f_y}{\partial S_{12}}, \frac{\partial f_y}{\partial S_{23}}, \frac{\partial f_y}{\partial S_{31}} \right)^T \quad (12)$$

In the next section we describe the modified Cam-clay material model and then derive the basic relations for stress integration, according to the above described computational procedure.

As it will be shown, the governing parameter "p" for the Cam-clay material is the increment of the mean plastic strain Δe_m^p. Further, in Section 3 we derive the elastic-plastic constitutive matrix for the both regimes shown in Fig. 1. The robustness, accuracy and efficiency of the developed computational algorithm is illustrated through numerical solutions obtained with the finite element package PAK [11]. One real, large scale footing problem, is solved, with the use of a contact procedure to model interaction between the structure and the soil.

2. Stress integration algorithm

We use the modified Cam-clay material according to [12], [13]. The material characteristics in plasticity domain are defined in the $\sqrt{3J_{2D}}$, σ_m plane by ellipses and by the critical state line, as shown in Figures 1 and 2. Material can have hardening, when during loading ellipses increase in size, or softening – corresponding to a decrease in the ellipse size. Hardening regime during time (load) step Δt is represented in Fig. 1 through two ellipses ${}^{t}f_y = 0$ and ${}^{t+\Delta t}f_y = 0$ at start and at end of time step. Softening regime in time step is schematically shown in Fig. 2, with ellipses ${}^{t+\Delta t}f_y = 0$ or ${}^{t+\Delta t}\overline{f}_y = 0$ smaller than the ellipse ${}^{t}f_y = 0$; details regarding this regime will be given further in the text. We consider that ellipses pass through the point A, displaced with respect to origin, for the hydrostatic tension T [6].

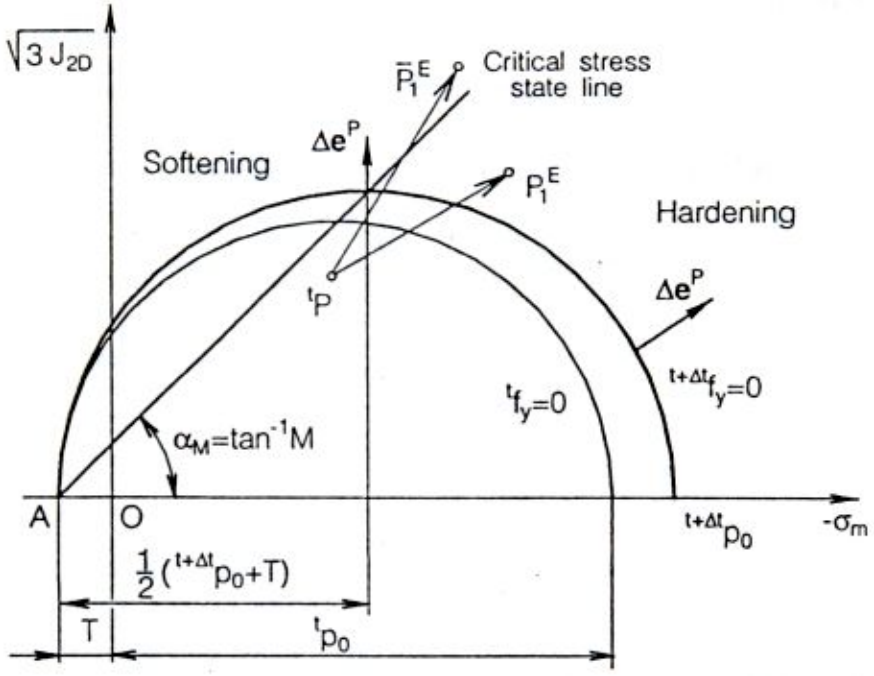

Figure 1. Modified Cam-clay model

We now present the basic relations for stress integration within the load (time) step Δt. First, we state that the elastic constitutive relations employed for this material are of the form

$$ {}^{t}\sigma_m = {}^{t}c_m \, {}^{t}e_m^E \tag{13} $$

$$ {}^{t}S_{ij} = \frac{1}{a_E} {}^{t}e_{ij}^E \tag{14} $$

where ${}^{t}\sigma_m$ and ${}^{t}S_{ij}$ are the mean and deviatoric stresses,

$$ {}^{t}\sigma_m = \frac{1}{3}\left({}^{t}\sigma_{11} + {}^{t}\sigma_{22} + {}^{t}\sigma_{33}\right) $$

$$ {}^{t}S_{ij} = {}^{t}\sigma_{ij} - {}^{t}\sigma_m \delta_{ij} \tag{15} $$

and ${}^t\sigma_{ij}$ are stress components, δ_{ij} - the Kronecker delta; ${}^te^E_m$ and ${}^te'^E_{ij}$ are the mean and deviatoric strains defined with respect to elastic strains ${}^te^E_{ij}$,

$$ {}^te^E_m = \frac{1}{3}{}^te^E_V = \frac{{}^te^E_{11} + {}^te^E_{22} + {}^te^E_{33}}{3} \tag{16} $$

$$ {}^te'^E_{ij} = {}^te^E_{ij} - {}^te^E_m\delta_{ij} \tag{17} $$

with ${}^te^E_V$ being the volumetric elastic strain; finally, $c_m = 3K$, where K is bulk modulus, and a_E is elastic constant related to the shear modulus G as $a_E = 0.5/G$. We consider that the bulk modulus can be either constant, or dependent of the mean stress and of the void ratio [2], [14], [15].

HardeningRegime. The yield condition of the material is defined as

$$ f_y = \left({}^t\sigma_m - \frac{{}^tp_o + T}{2}\right)^2 - \left(\frac{{}^tp_o - T}{2}\right)^2 + \frac{3\,{}^tJ_{2D}}{M^2} = 0 \tag{18} $$

where

$$ {}^tJ_{2D} = \frac{1}{2}{}^tS_{ij}\,{}^tS_{ij} \tag{19} $$

is the second invariant of the stress deviator, M is material constant and ${}^tp_o$ is the hardening parameter. This parameter defines the ellipse size, as shown in Fig. 1, and its change can be related to the change of the plastic volumetric strain de^P_V, as

$$ \frac{dp_o}{{}^tp_o} = -\frac{1 + {}^te}{k_s}de^P_V \tag{20} $$

where ${}^te$ is the void ratio and $k_s = \lambda - \kappa$, and λ and κ are usual material constants. The void ratio can be obtained from the volumetric strain from the relation

$$ {}^te = (1 + {}^oe)e^{{}^te_V} - 1 \tag{21} $$

where ${}^oe$ is the initial void ratio.

Suppose that stress state at time t is given by a point ${}^tP$ in the elastic region. Due to strain increment at the material point we have a change of stresses. We first calculate trial elastic stresses employing (13) and (14),

$$ {}^{t+\Delta t}\sigma^E_m = {}^tc_m\,{}^{t+\Delta t}e''_m \tag{22} $$

$$ {}^{t+\Delta t}S^E_{ij} = \frac{1}{a_E}{}^{t+\Delta t}e''_{ij} \tag{23} $$

where

$$ {}^{t+\Delta t}e''_m = {}^{t+\Delta t}e_m - {}^{t+\Delta t}e^p_m \tag{24} $$

$$ {}^{t+\Delta t}e''_{ij} = {}^{t+\Delta t}e'_{ij} - {}^{t+\Delta t}e'^p_{ij} \tag{25} $$

Here ${}^{t+\Delta t}e_m$ and ${}^{t+\Delta t}e'_{ij}$ are the mean and deviatoric strains (considered known in the strain driven problems); ${}^{t+\Delta t}e^p_m$ and ${}^{t+\Delta t}e'^p_{ij}$ are plastic mean and plastic

deviatoric strains at start of time step. Substituting ${}^{t+\Delta t}\sigma_m^E$ and ${}^{t+\Delta t}S_{ij}^E$ into (18) we calculate ${}^{t+\Delta t}f_y^E$. In case ${}^{t+\Delta t}f_y^E \leq 0$, there is no plastic deformation in the time step, and ${}^{t+\Delta t}\sigma_m^E$ and ${}^{t+\Delta t}S_{ij}^E$ are the solutions for stresses. Otherwise, we proceed to plasticity calculations as follows. We first suppose that elastic stress state corresponds to either point P_1^E or $\overline{P}_1^E$ (to the right from vertical line $({}^tp_o + T)/2$) in Fig. 1.

Due to plastic flow in time step Δt we have increments of the mean and deviatoric plastic strains Δe_m^p and Δe_{ij}^p. Substituting Δe_m^p and Δe_{ij}^p into (22) and (23) we obtain

$$ {}^{t+\Delta t}\sigma_m = {}^tc_m \left({}^{t+\Delta t}e_m'' - \Delta e_m^p \right) \tag{26} $$

$$ {}^{t+\Delta t}S_{ij} = \frac{1}{a_E} \left({}^{t+\Delta t}e_{ij}'' - \Delta e_{ij}^p \right) \tag{27} $$

Further we employ the flow rule (8) with the yield function ${}^{t+\Delta t}f_y$,

$$ {}^{t+\Delta t}f_y = \left({}^{t+\Delta t}\sigma_m - \frac{{}^{t+\Delta t}p_o + T}{2} \right)^2 - \left(\frac{{}^{t+\Delta t}p_o - T}{2} \right)^2 + \frac{3\,{}^{t+\Delta t}J_{2D}}{M^2} = 0 \tag{28} $$

Hence, according to (9) we obtain

$$ \Delta e_{ij}^p = \frac{\Delta\lambda}{3} \left(2\,{}^{t+\Delta t}\sigma_m - {}^{t+\Delta t}p_o \right) \delta_{ij} + \frac{3\Delta\lambda}{M^2} {}^{t+\Delta t}S_{ij} \tag{29} $$

and then

$$ \Delta e_m^p = \frac{\Delta\lambda}{3} \left(2\,{}^{t+\Delta t}\sigma_m - {}^{t+\Delta t}p_o - T \right) \tag{30} $$

$$ \Delta e_{ij}^p = \frac{\Delta\lambda}{M^2} {}^{t+\Delta t}S_{ij} \tag{31} $$

where $\Delta\lambda$ is a positive scalar to be determined. Substituting (31) into (27) we solve for ${}^{t+\Delta t}S_{ij}$,

$$ {}^{t+\Delta t}S_{ij} = \frac{{}^{t+\Delta t}e_{ij}''}{a_E + 3\Delta\lambda/M^2} \tag{32} $$

Next, we employ the relation (20) and express the hardening parameter in the form

$$ {}^{t+\Delta t}p_o = {}^tp_o\, \mathrm{e}^{-\frac{\Delta e_m^p}{{}^{t+\Delta t}b_V}} \tag{33} $$

where

$$ {}^{t+\Delta t}b_V = \frac{k_s}{3(1 + {}^{t+\Delta t}e)} \tag{34} $$

is a known constant. We mention here that instead of (33), an equivalent relation can be used,

$$ {}^{t+\Delta t}p_o = \mathrm{e}^{\frac{e_1 - {}^{t+\Delta t}e}{k_s}} \, {}^{t+\Delta t}\sigma_m^{-\frac{\kappa}{k_s}} \tag{33a} $$

which follows from the model definition, where e_1 corresponds to $\sigma_m = 1$ on the line of normal consolidation (LNC line). We will further use the relation (33).

By inspecting expressions (32) for ${}^{t+\Delta t}S_{ij}$, (26) for ${}^{t+\Delta t}\sigma_m$ and (33) for ${}^{t+\Delta t}p_o$, and with use of (30), we conclude that ${}^{t+\Delta t}S_{ij}$, ${}^{t+\Delta t}\sigma_m$, ${}^{t+\Delta t}p_o$ and $\Delta\lambda$ can be considered as functions of one parameter – the increment of the mean plastic strain Δe_m^P. Hence, in accordance with the GPM described in Section 1, we have that the governing parameter is Δe_m^P. To determine Δe_m^P corresponding to given strains ${}^{t+\Delta t}e_{ij}$ at the end of a load step and given stress/strain state at the start of a load step, expressed through ${}^{t}e_{ij}^P$ and ${}^{t}p_o$, we impose the condition (28). With use of definition of the second invariant ${}^{t+\Delta t}J_{2D}$, ${}^{t+\Delta t}J_{2D} = \frac{1}{2}{}^{t+\Delta t}S_{ij}\,{}^{t+\Delta t}S_{ij}$, we write the yield condition (28) in the form

$$
{}^{t+\Delta t}f_y = \left({}^{t+\Delta t}\sigma_m - \frac{{}^{t+\Delta t}p_o - T}{2}\right)^2 + \left(\frac{{}^{t+\Delta t}p_o - T}{2}\right)^2 + \\
+ \frac{3\,d^2}{2M^2\left(a_E + \dfrac{3\Delta\lambda}{M^2}\right)^2} = 0 \tag{35}
$$

where

$$
{}^{t+\Delta t}d^2 = {}^{t+\Delta t}e''_{ij}\,{}^{t+\Delta t}e''_{ij} \tag{36}
$$

is a known quantity.

With Δe_m^P computed as the solution of (35) we also have ${}^{t+\Delta t}\sigma_m$ from (26), ${}^{t+\Delta t}p_o$ – from (33) and $\Delta\lambda$ – from (30). Then, we finally calculate ${}^{t+\Delta t}S_{ij}$ from (32) and ${}^{t+\Delta t}e_{ij}^P$ from (31). The computational steps are summarized in Table 1.

From the above we conclude that the problem of stress integration is reduced to solving the nonlinear equation (35), or to finding the zero of the function ${}^{t+\Delta t}f_y(\Delta e_m^P)$, which is in accordance with the steps 1 to 3 of the GPM given in Section 1. It is interesting to note that the function ${}^{t+\Delta t}f_y(\Delta e_m^P)$ is a monotonic increasing function, for any increment Δe_m^P, as shown in Table 3 and in Ref. [10] for other material models. Also, the computational procedure is simple, efficient and reliable, confirming the robustness of the algorithm; these characteristics are illustrated in Example 1. Also, we point out that all fundamental elastic-plastic relations are satisfied exactly. The only approximation of the algorithm lies in the relation (29). Comparing to the procedure in Ref. [14], we emphasize that our algorithm is computationally efficient and does not need a double iteration loop in solving the governing equation (35). The efficiency of the algorithm is extremely important in practical applications. For example, in the finite element analysis, the history of plastic deformation is traced in every integration point whose number may reach over tens of thousands for a real engineering problem. Then, the solution time is drastically reduced if we have one iteration loop instead of two (for example, instead $10 \times 10 = 100$ trial solutions, we have only 10 trials at each integration point).

In comparison with the "closest point projection" procedures (ex. Refs. [6], [7]) the proposed procedure is more efficient, since it operates on one nonlinear equation instead of a Newton iteration loop for solution of linearized set of six equations; and, more significantly, the GPM provides solution even for large strain increments (illustrated in Example 1).

The above procedure is implicit and possesses superiority regarding accuracy of solutions when compared to the explicit algorithms [5], [10]. The solution accuracy is illustrated here in Example 1.

Finally in this section we analyze the deformation corresponding to the softening conditions.

Softening conditions. When the trial elastic state is given by point P_2^E (on the left – with a selected tolerance, from the vertical line $({}^tp_o + T)/2$) in Fig. 2, material deforms plastically in time step, leading to softening, as previously described.

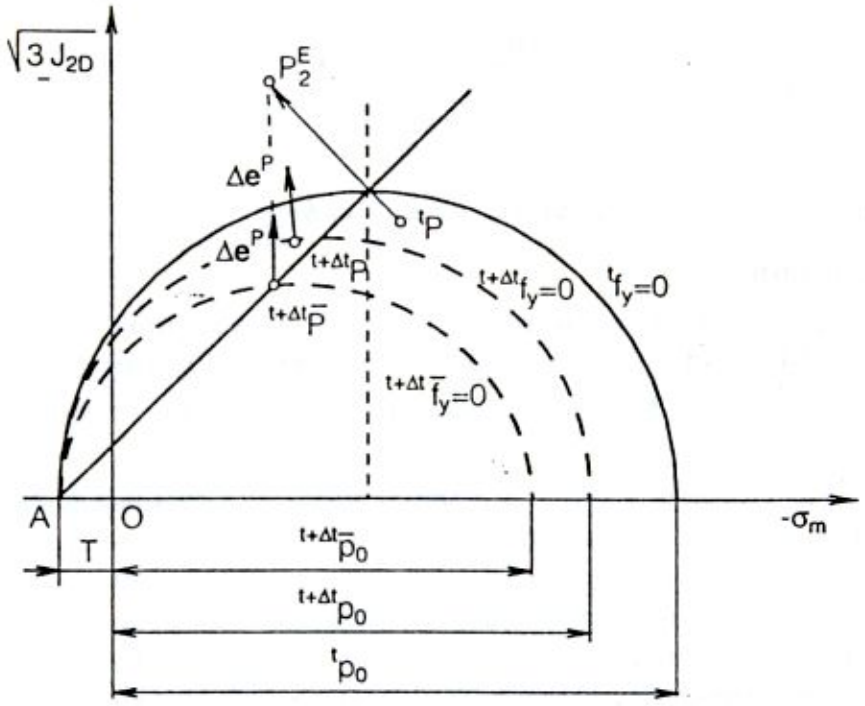

Figure 2. Softening regime in time step

Here, we can take two approaches. One is to consider the elliptical yield surface as the plastic potential, with $\Delta \mathbf{e}^P$ having tensile mean plastic strain increment Δe_m^P, as shown in Fig. 2 (stress point ${}^{t+\Delta t}P$ on the yield surface ${}^{t+\Delta t}f_y = 0$). Then, all relations derived for the hardening regime are applicable, and we do not further discuss this concept here. We will comment numerical results based on this approach in Example 2.

Another approach is to consider that the elastic region is bounded by the critical state line and by part of ellipses below the critical state line. Then, we take that the yielding occurs at the critical stress state (CSS) line. We mention here that we also consider that the yielding is at CSS line when the trial elastic

state lies, within a selected tolerance, on the vertical line $({}^{t}p_o + T)/2$.

We further present the basic relations for stress integration in case of yielding on the CSS line. As shown in Fig. 2, we suppose that yielding in time step Δt corresponds to point ${}^{t+\Delta t}\overline{P}$ on the vertical line passing through ${}^{t+\Delta t}P_2^E$. Namely, we impose the condition

$$\Delta e_m^P = 0 \tag{37}$$

which corresponds to yielding on the ellipse ${}^{t+\Delta t}\overline{f}_y = 0$, with horizontal tangent at point ${}^{t+\Delta t}\overline{P}$. With the condition (37) we obtain from (26)

$${}^{t+\Delta t}\sigma_m = {}^{t}c_m \, {}^{t+\Delta t}e_m'' \tag{38}$$

and also

$${}^{t+\Delta t}p_o = 2\,{}^{t+\Delta t}\sigma_m - T \tag{39}$$

We have the softening of the material in the current load step, since the yield ellipse ${}^{t+\Delta t}\overline{f}_y = 0$, corresponding to ${}^{t+\Delta t}\overline{p}_o$, is inside the yield curve ${}^{t}f_y = 0$. We mention that the ellipse ${}^{t+\Delta t}\overline{f}_y = 0$ is uniquely defined by ${}^{t+\Delta t}\sigma_m$ (i.e. by strain ${}^{t+\Delta t}e_m''$).

The yielding at point ${}^{t+\Delta t}\overline{P}$ is in accordance with conditions of perfect plasticity [10]. Hence, we have increments of deviatoric plastic strains only, defined by (31). We obtain the value of $\Delta\lambda$ by substituting (39) into (35), i.e.

$$\Delta\lambda = \frac{M^2}{3}\left(\frac{\sqrt{2}\,{}^{t+\Delta t}d}{2M\,|{}^{t+\Delta t}\sigma_m - T|} - a_\varepsilon\right) \tag{40}$$

With this $\Delta\lambda$ we calculate ${}^{t+\Delta t}S_{ij}$ from (32) and $\Delta e_{ij}'$ from (31). Also, we update the hardening parameter using (39) for calculations in the next load step.

3. Elastic–plastic constitutive matrix

In order to have high convergence rate in the Newton iterative solution scheme [1], [10], it is necessary to determine the tangent constitutive relations. Here we derive the elastic-plastic constitutive matrix following the general concept given in Section 1, and by using expressions for stresses presented above.

First, for ease of writing we introduce the one-index notation for stresses and strains, for example

$$\begin{gathered}\sigma_1 = \sigma_{11}, \quad \sigma_2 = \sigma_{22}, \ldots \quad \sigma_6 = \sigma_{31} \\ e_1 = e_{11}, \quad e_2 = e_{22}, \ldots, \quad e_6 = \gamma_{31} = 2\,e_{31}\end{gathered} \tag{41}$$

Table 1. Solution steps in stress integration

1. Calculate trial elastic stresses

$$^{t+\Delta t}\sigma_m^E = {}^t c_m \, {}^{t+\Delta t}e''_m$$

$$^{t+\Delta t}S_{ij}^E = \frac{1}{a_E} {}^{t+\Delta t}e''_{ij}$$

If $^{t+\Delta t}f_y \left(^{t+\Delta t}\sigma_m^E, \, ^{t+\Delta t}S_{ij}^E \right) \leq 0$, deformation is elastic – go to next load step.

2. Deformation is plastic, hardening regime:

Start with $\Delta e_m^P = 0$

$$^{t+\Delta t}\sigma_m^{(k)} = {}^t c_m \left(^{t+\Delta t}e''_m - \Delta e_m^{P(k)} \right)$$

$$^{t+\Delta t}p_o^{(k)} = {}^t p_o \, \mathrm{e}^{-3\frac{1+{}^{t+\Delta t}e}{k_s}\Delta e_m^{P(k)}}$$

$$\Delta\lambda^{(k)} = \frac{3\Delta e_m^{P(k)}}{2\,{}^{t+\Delta t}\sigma^{(k)} - {}^{t+\Delta t}p_o^{(k)} - T}$$

$$f_y^{(k)} = f_y \left(^{t+\Delta t}\sigma_m^{(k)}, \, ^{t+\Delta t}p_o^{(k)}, \, \Delta\lambda^{(k)} \right)$$

$$\Delta e_m^{P(k+1)} = \Delta e_m^{P(k)} - \frac{f_y^{(k)}}{\partial f_y^{(k)} / \partial(\Delta e_m^P)}$$

Iterate on $\Delta e_m^{P(k+1)}$ until

$$^{t+\Delta t}f_y = \left(^{t+\Delta t}\sigma_m - \frac{^{t+\Delta t}p_o - T}{2} \right)^2 - \left(\frac{^{t+\Delta t}p_o - T}{2} \right)^2 + \frac{3\,d^2}{2M^2 \left(a_E + \frac{3\Delta\lambda}{M^2} \right)} = 0$$

$$\Delta e_m^P = \Delta e_m^{P(k)}$$

Calculate final values for $^{t+\Delta t}S_{ij}$, $^{t+\Delta t}e_{ij}^{'P}$ using (32) and (31). Update value of the hardening parameter.

3. Critical stress state

Calculate $\Delta\lambda$ as

$$\Delta\lambda = \frac{M^2}{3} \left(\frac{\sqrt{2}\,{}^{t+\Delta t}d}{2M \left| ^{t+\Delta t}\sigma_m - T \right|} - a_E \right)$$

and final values for $^{t+\Delta t}S_{ij}$ from (32) and $\Delta e_{ij}^{'P}$ from (31). Update value of the hardening parameters.

We use here engineering instead of tensorial components for strains, as indicated above. With the above notation we express stresses as

$$\begin{aligned} {}^{t+\Delta t}\sigma_i &= {}^{t+\Delta t}S_i + {}^{t+\Delta t}\sigma_m \quad i = 1,2,3 \\ {}^{t+\Delta t}\sigma_i &= {}^{t+\Delta t}S_i \qquad\qquad\quad i = 4,5,6 \end{aligned} \tag{42}$$

Since deviatoric stresses ${}^{t+\Delta t}S_i$ and the mean stress ${}^{t+\Delta t}\sigma_m$ are functions of deviatoric strains ${}^{t+\Delta t}e_j'$ and the mean strain ${}^{t+\Delta t}e_m$, we express components ${}^{t+\Delta t}C_{ij}^{EP}$ of the elastic-plastic matrix as

$${}^{t+\Delta t}C_{ij}^{EP} = \frac{\partial^{t+\Delta t}\sigma_i}{\partial^{t+\Delta t}e_j} = \overline{C}_{ik}\frac{\partial^{t+\Delta t}e_k'}{\partial^{t+\Delta t}e_j} + \frac{1}{3}C_{ij}^m \tag{43}$$

where

$$\overline{C}_{ik} = \overline{C}_{ik}' + \overline{C}_{ik}^{,m} \tag{44}$$

$$C_{ik}^m = \hat{C}_{ij}^{,m} + \hat{C}_{ij}^m \tag{45}$$

and summation over dummy index k is implied; also we have used relation of the form (16) for the mean strain ${}^{t+\Delta t}e_m$, from which follows

$$\frac{\partial^{t+\Delta t}e_m}{\partial^{t+\Delta t}e_j} = \frac{1}{3} \quad j = 1,2,3 \tag{46}$$

The expressions for components in (44)and (45) are

$$\overline{C}_{ik}' = \frac{\partial^{t+\Delta t}S_i}{\partial^{t+\Delta t}e_m''} \qquad i,k = 1,2,\ldots,6 \tag{47}$$

$$\begin{aligned} \overline{C}_{ik}^{,m} &= \frac{\partial^{t+\Delta t}\sigma_m}{\partial^{t+\Delta t}e_m''} \qquad \begin{aligned} i &= 1,2,3 \\ k &= 1,2,\ldots,6 \end{aligned} \end{aligned} \tag{48}$$

$$\begin{aligned} \overline{C}_{ik}^{,m} &= 0 \qquad\qquad \begin{aligned} i &= 4,5,6 \\ k &= 1,2,\ldots,6 \end{aligned} \end{aligned} \tag{49}$$

and

$$\begin{aligned} \hat{C}_{ij}^{,m} &= \frac{\partial^{t+\Delta t}S_i}{\partial^{t+\Delta t}e_m''} \qquad \begin{aligned} i &= 1,2,\ldots,6 \\ j &= 1,2,3 \end{aligned} \\ \hat{C}_{ij}^{,m} &= 0 \qquad\qquad j = 4,5,6 \end{aligned} \tag{50}$$

$$\begin{aligned} \hat{C}_{ij}^m &= \frac{\partial^{t+\Delta t}\sigma_m}{\partial^{t+\Delta t}e_m''} \qquad i,j = 1,2,3 \\ \hat{C}_{ij}^m &= 0 \qquad\qquad \begin{aligned} i &= 1,2,3 \quad j = 4,5,6 \\ i &= 4,5,6 \quad j = 1,2,\ldots,6 \end{aligned} \end{aligned} \tag{51}$$

In the above expressions for $\overline{C}'_{ik}$, $\overline{C}'^{,m}_{ik}$, $\hat{C}'^{,m}_{ij}$ and $\hat{C}'^{m}_{ij}$ we have taken into account the relations

$$\frac{\partial^{t+\Delta t}e''_i}{\partial^{t+\Delta t}e'_j} = \delta_{ij}$$

$$\frac{\partial^{t+\Delta t}e''_m}{\partial^{t+\Delta t}e_m} = 1 \qquad \text{no sum on m} \tag{52}$$

which follow from (25) and (24). We now proceed to determine derivatives indicated in (47) to (51).

From (32) follows

$$\overline{C}'_{ik} = \frac{\delta_{ik}}{a_E + 3\Delta\lambda/M^2} - \frac{{}^{t+\Delta t}e''_i}{M^2\,(a_E + 3\Delta\lambda/M^2)^2}\Delta\lambda_{,k} \tag{53}$$

where $\Delta\lambda_{,k}$ is used for $\partial(\Delta\lambda)/\partial^{t+\Delta t}e''_k$. In case of the CSS regime we obtain from (40) that

$$\Delta\lambda_{,k} = l_1\,{}^{t+\Delta t}\hat{e}''_k \tag{54}$$

where

$$l_1 = -\frac{\sqrt{2}\,M}{6\,({}^{t+\Delta t}\sigma_m - T)\,{}^{t+\Delta t}d} \tag{55}$$

$${}^{t+\Delta t}\hat{e}''_k = {}^{t+\Delta t}e''_k \qquad k = 1,2,3$$

$${}^{t+\Delta t}\hat{e}''_k = 2\,{}^{t+\Delta t}e''_k \qquad k = 4,5,6 \tag{56}$$

In case of hardening regime, or for softening with yielding on the ellipse, we have from (30) that

$$\Delta\lambda_{,k} = \frac{\Delta\lambda}{\Delta e^P_m}\left[\Delta e^P_{m,k} - \frac{\Delta\lambda}{3}\,(2\,{}^{t+\Delta t}\sigma_{m,k} - {}^{t+\Delta t}p_{o,k})\right] \tag{57}$$

where $\Delta e^P_{m,k}$, ${}^{t+\Delta t}\sigma_{m,k}$ and ${}^{t+\Delta t}p_{o,k}$ are derivatives of Δe^P_m, ${}^{t+\Delta t}\sigma_m$ and ${}^{t+\Delta t}p_o$ with respect to ${}^{t+\Delta t}e''_k$. These derivatives can be calculated from expressions (26); (33) or (33a); and (35) – which, according to (6), must be differentiated with respect to ${}^{t+\Delta t}e''_k$. The resulting expression for $\overline{C}'_{ik}$ has a matrix form convenient for applications,

$$\overline{C}'_{ik} = \frac{\delta_{ik}}{a_E + 3\Delta\lambda/M^2} - l_2\,{}^{t+\Delta t}e''_i\,{}^{t+\Delta t}\hat{e}''_k \tag{58}$$

where the coefficient l_2 contains known quantities $\Delta\lambda$, Δe^P_m, ${}^{t+\Delta t}d$, ${}^{t+\Delta t}\sigma_m$ and ${}^{t+\Delta t}p_o$; and elastic constants a_E and ${}^{t}c_m$.

Similarly, coefficients $\overline{C}_{ik}^{,m}$ follow from (26) and (35),

$$\overline{C}_{ik}^{,m} = -\frac{{}^{t}c_m}{l_3}\,{}^{t+\Delta t}\hat{e}_k'' \tag{59}$$

where l_3 is known coefficient as l_2.

Finally, we calculate derivatives with respect to ${}^{t+\Delta t}e_m''$, indicated in (50) and (51). From (32) and (26) we obtain

$$\hat{C}_{ij}^{,m} = -\frac{3\,{}^{t+\Delta t}e_i''}{M^2\left(a_g + 3\,\Delta\lambda/M^2\right)^2}\,\frac{\partial(\Delta\lambda)}{\partial^{t+\Delta t}e_m''} \tag{60}$$

$$\hat{C}_{ij}^{m} = {}^{t}c_m\left[1 - \frac{\partial(\Delta e_m)}{\partial^{t+\Delta t}e_m''}\right] \tag{61}$$

First, the simpler case is the CSS regime when, according to (40) and (37), we have

$$\begin{aligned} \hat{C}_{ij}^{,m} &= 0 \\ \hat{C}_{ij}^{m} &= {}^{t}c_m \end{aligned} \tag{62}$$

In case of the hardening regime, or in case of softening with yielding on the ellipse, in order to calculate derivatives $\partial(\Delta\lambda)/\partial^{t+\Delta t}e_m''$ and $\partial(\Delta e_m^P)/\partial^{t+\Delta t}e_m''$ we follow the procedure shown above for determination of derivatives with respect to ${}^{t+\Delta t}e_k''$. After some algebra we obtain

$$\begin{aligned} \hat{C}_{ij}^{,m} &= -l_4\,{}^{t+\Delta t}e_i'' \\ \hat{C}_{ij}^{m} &= {}^{t}c_m(1 - l_5) \end{aligned} \tag{63}$$

where l_4 and l_5 are the coefficients expressed in terms of the same quantities as l_2 in (58).

The derived expressions for ${}^{t+\Delta t}C_{ij}^{EP}$ contain tangent moduli corresponding to end of time step. They are obtained by a consistent differentiation of the governing relations for stress integration. We illustrate the tangent character of ${}^{t+\Delta t}\mathbf{C}^{EP}$ on numerical examples.

4. Examples

With the examples we verify the accuracy of the presented stress integration algorithm and demonstrate the applicability of the algorithm to one interesting engineering problem. Also, with use of the general purpose finite element program for nonlinear analysis PAK [11], we follow history of deformation up to the collapse of the material.

Example 1. Critical state model for laboratory specimen. We model triaxial test by one 3-D solid element. The two principal stresses are held constant, $\sigma_2 = \sigma_3 = 100\ kN/m^2$, while σ_1 is increased. Material data are given in the Fig. 3(a), according to Ref. [2]. The dependence of stress difference $\sigma_1 - \sigma_2$ on the axial strain is shown in Fig. 3(a), which is the same as in Ref. [2]. We have solved this example by using the full-Newton method with line search and the BFGS method. In order to apply the arc-length method we have modeled the constant stress condition $\sigma_2 = \sigma_3$ with lateral rigid-perfectly plastic trusses; the computed axial stress-displacement relations are plotted in Fig. 3(b).

(a) (b)

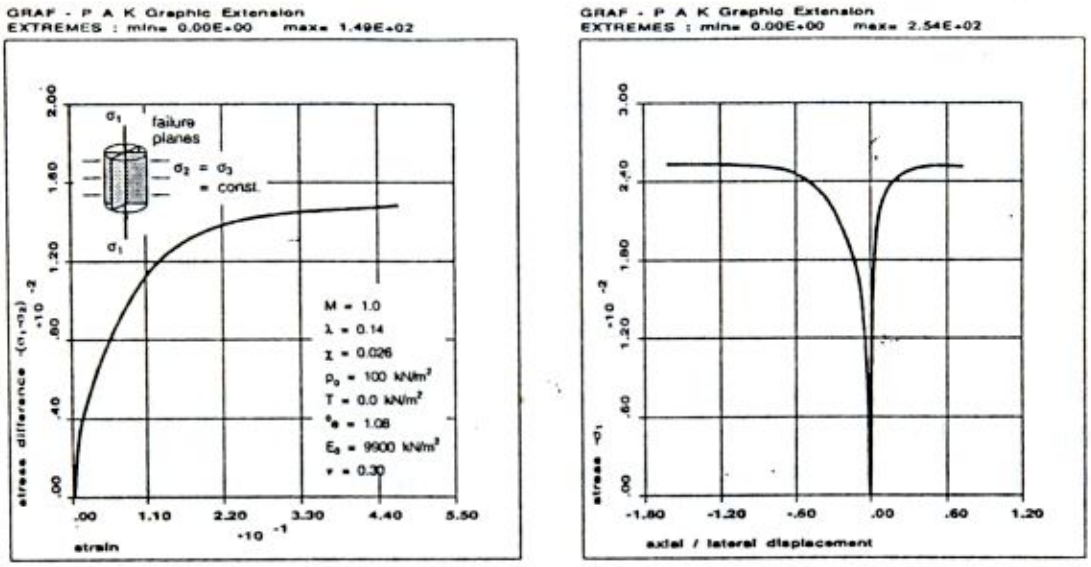

Figure 3 Triaxial test modeled by
one 3-D solid element
(a) stress difference $\sigma_1 - \sigma_2$ versus
axial strain
(b) axial stress-displacement relations

To illustrate the robustness and accuracy of the proposed algorithm, in Table 2 we give results corresponding to final value of axial stress $\sigma_1 = 180\ kN/m^2$, for various number of load steps. It can be seen from the table that results are accurate enough even for two steps only.

Error in the axial strain e_1 and in volumetric plastic strain e^P with respect to 100-step solution is graphically shown in Fig. 4(a) and (b). We note that error in e_V^P is very small for large load (strain) increment, while the error in e_1 is significantly larger (but decreases rapidly with number of steps N). Larger error in e_1 and other strain components, which also can be seen from Table 2, is due to the fact that the normal to the yield surface changes significantly during plastic flow.

Table 2. Fiual values for various number of solution steps

Variable	Number of steps		
	100	10	2
e_1	-5.522×10^{-2}	-5.797×10^{-2}	-7.172×10^{-2}
$e_1 = e_3$	3.921×10^{-2}	5.274×10^{-2}	1.197×10^{-3}
e_V^P	-1.068×10^{-2}	-1.070×10^{-2}	-1.081×10^{-2}
e_1^P	-4.316×10^{-2}	-4.591×10^{-2}	-5.964×10^{-2}
$e_1^P = e_3^P$	5.556×10^{-3}	6.907×10^{-3}	1.361×10^{-2}
p_o	-176.3	-176.3	-176.6

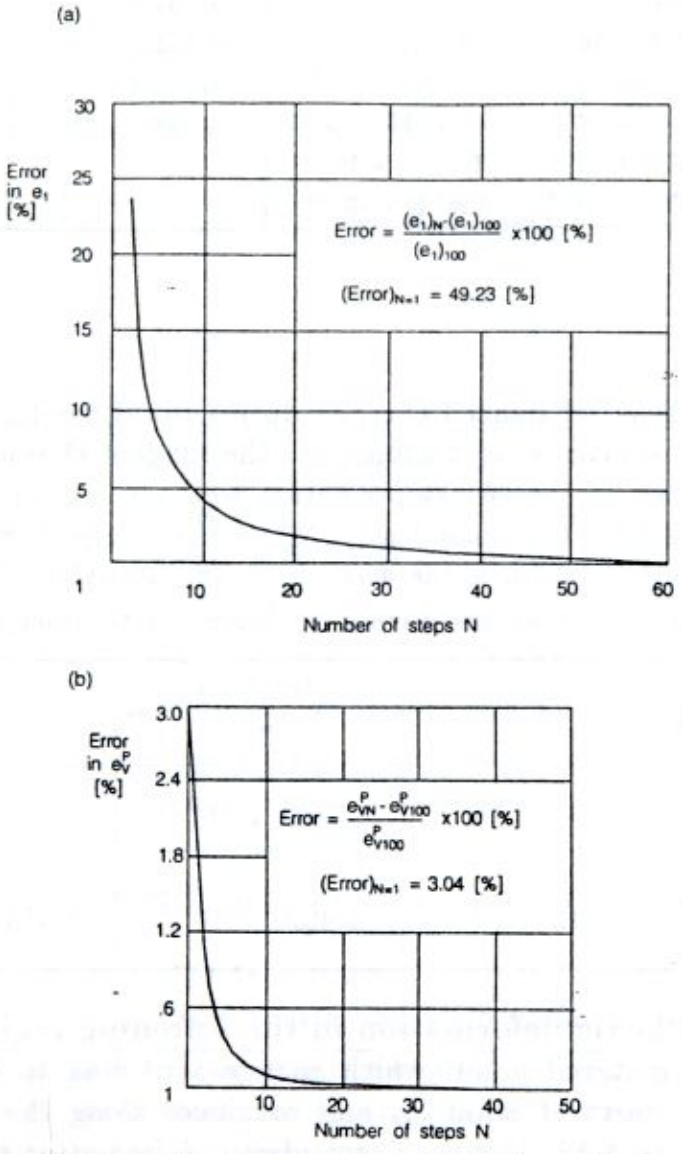

Figure 4 Error in terms of number of steps
a) Error in axial strain e_1
(b) Error in volumetric plastic strain e_V^P

Illustration of robustness and numerical efficiency is given through Table 3. We see that the function $f_y(\Delta e_m^P)$ is monotonic for the 2-step and 10-step solutions and that the zero of the function is obtained by Newton iterations with just several trials.

Tabele 3. Function $f(\Delta e_m^P)$ during Newton iteration solution procedure

2-step solution 2-nd, 4-th iteration			10-step solution 10-th step, 3-rd iteration	
Trial number	Δe_m^P	f_y	Δe_m^P	f_y
1	-0.25839×10^{-2}	0.20645×10^{6}	-0.70346×10^{-3}	0.19016×10^{5}
2	-0.40544×10^{2}	0.56843×10^{5}	-0.93040×10^{-3}	0.37900×10^{4}
3	-0.46810×10^{-2}	0.13262×10^{5}	-0.95374×10^{-3}	0.32394×10^{3}
4	-0.48237×10^{-2}	0.20814×10^{4}	-0.95398×10^{-3}	0.32452×10^{1}
5	-0.48314×10^{-2}	0.10243×10^{3}	-0.95398×10^{-3}	0.33734×10^{-3}
6	-0.48315×10^{-2}	0.30196×10^{0}	-0.95398×10^{-3}	0.26623×10^{-11}
7	-0.48315×10^{-2}	0.26539×10^{-5}	-	-
8	-0.48315×10^{-2}	0.26539×10^{-12}	-	-

In Table 4 we give unbalanced energies during iterations for the last step, of the 100-and 10-step solutions, to demonstrate the tangent character of ${}^{t+\Delta t}\mathbf{C}^{EP}$. We mention that even in the two-step solution we have 3 iterations for the first step, and 4 iterations for the second step, when the strain increments are quite large and the starting solution is far away from the actual solution.

Table 4. Unbalanced energies during iterations in the last step

	Iteration		
	1	2	3
100-step solution	2.6107×10^{-5}	5.7838×10^{-10}	-
10-step solution	1.2413×10^{-2}	1.4027×10^{-4}	1.5132×10^{-7}

Example 2. Plastic deformation in the softening regime. We prescribe strains at a material point, which change according to diagrams in Fig. 4(a). The yielding starts at point A_o and continues along the hydrostatic axis up to the point A_1 (see Fig. 5(b)). Then, plastic deformation from point A_1 to point A_2 corresponds to the hardening regime, while from A_3 the material has softening behavior. The final point A_4 is obtained by employing the ellipse as the plastic potential, and the point $\overline{A}_4$ is reached following softening according to the CSS conditions.

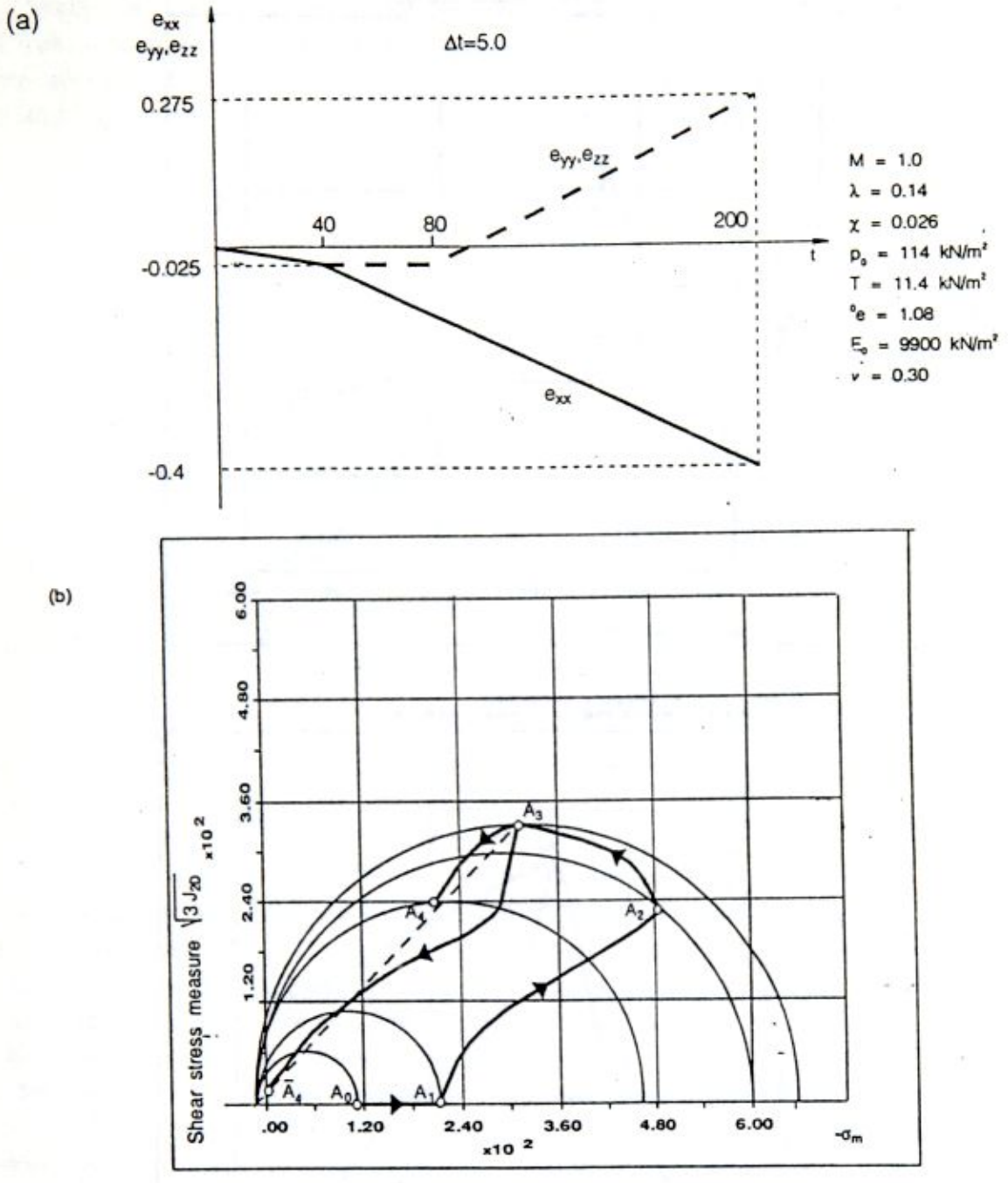

Figure 5 Straining which produces hardening and softening of the material
(a) Strain history
(b) Stress path and yield surfaces

In Figs. 6 (a) and (b) we give solutions for the mean stress σ_m and for $\sqrt{3J_{2D}}$ in terms of axial strain, using the above described two approaches for stress integration. It can be seen from diagrams that the softening is much sharper when stress calculation is performed according to the CSS conditions. Since the authors do not have the adequate experimental results, the results in Fig. 6 are given to qualitatively demonstrate the model behavior under softening conditions.

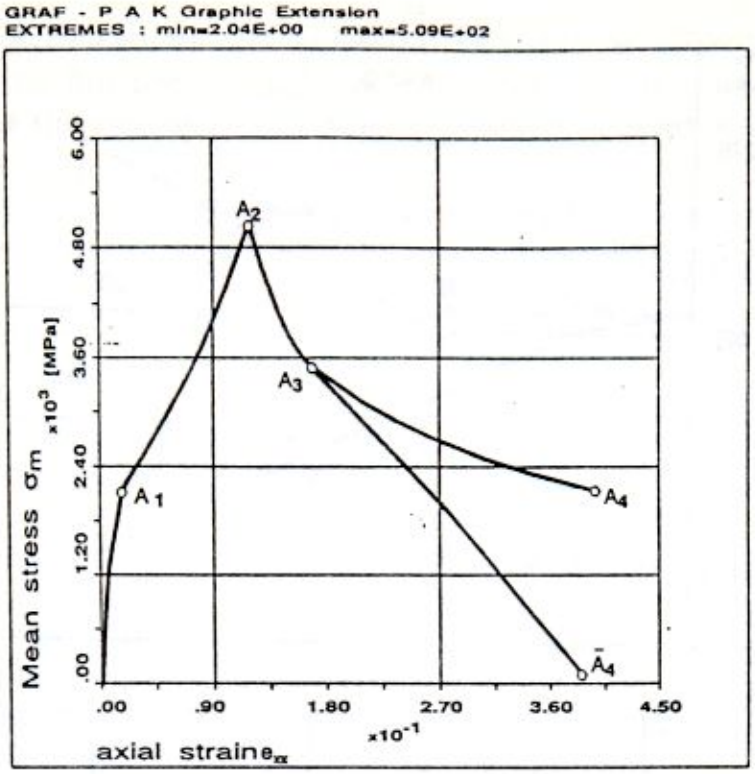

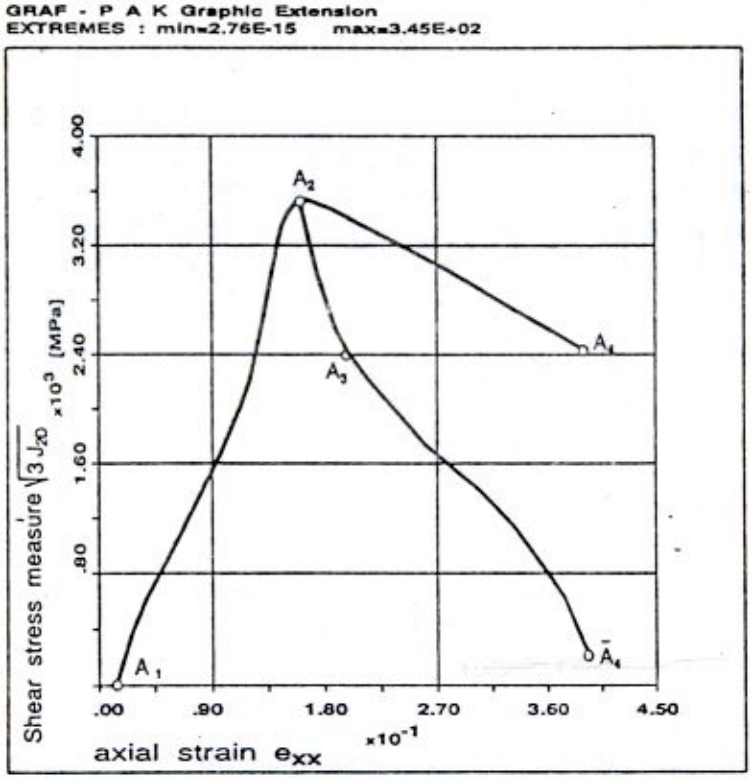

Figure 6. Material response under softening conditions
(a) Dependence of the mean stress on axial strain
(b) Dependence of shear stress measure $\sqrt{3J_{2D}}$ on axial strain

Finally, in Fig. 7 we give the material response in case of the yielding at CSS line, which corresponds to the perfect plasticity conditions. Material data are as given in Fig. 5(a). We follow loading conditions up to point A_2 in Fig. 5(b) and then keep volumetric strain constant until the CSS line is reached.

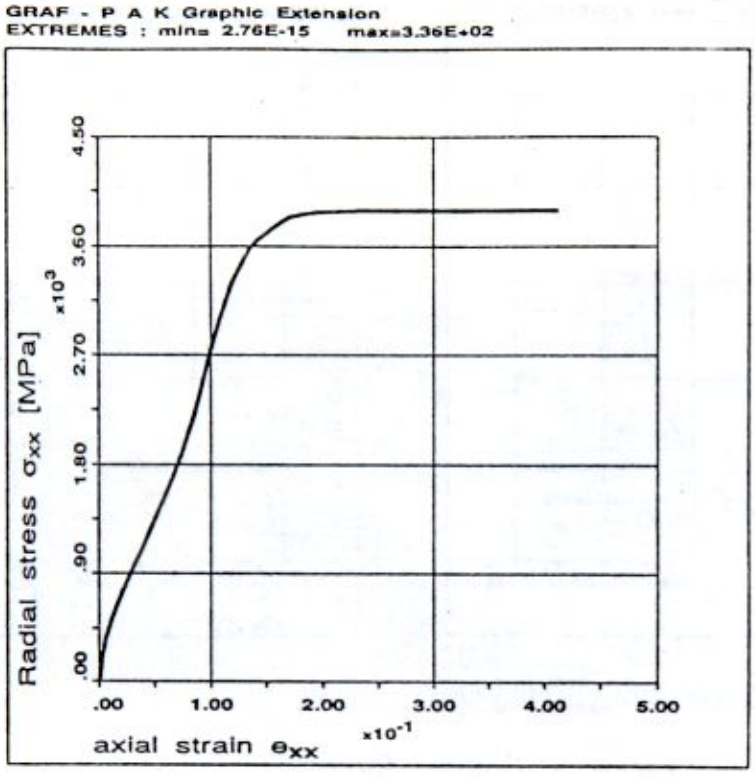

Figure 7. Yielding of material on the CSS line

Example 3. Strip footing problem. The footing problem, shown in Fig. 8 is modeled with 450 2-D plane strain elements for soil part and 10 elements for the rigid foot. Total number of nodes is 518. At the start of analysis foot and soil are separated bodies. The surface loading $p_o = 22.33\,kN/m^2$ is applied in the first step, and E remains the same during the analysis. In the second step foot and soil come into the contact through the prescribed displacements of the foot. In the next steps the incremental displacement is applied to the foot so that the total displacement increment in these steps is $0.15\,m$.

Full Newton iteration method with line search is applied. We have used variable bulk modulus, expressed as

$$ {}^t c_m = 3\,{}^t K = -\frac{1+{}^t e}{\kappa}\,{}^t \sigma_m $$

In each step we have used the bulk modulus corresponding to the strain and stress at the start of the step. Material data are as follows:

$$ \begin{array}{lcllcl} M & = & 1.4 & E_o & = & 9900\,kN/m^2 \\ \lambda & = & 0.37 & \nu & = & 0.35 \\ \kappa & = & 0.054 & & & \\ p_o & = & -4. & & & \\ {}^o e & = & 2.58 & & & \end{array} $$

We have used the initial Young's modulus E_o in the first step only. The total width of the analyzed soil is $21\,m$, the depth is $9\,m$, and the foot width is $3\,m$.

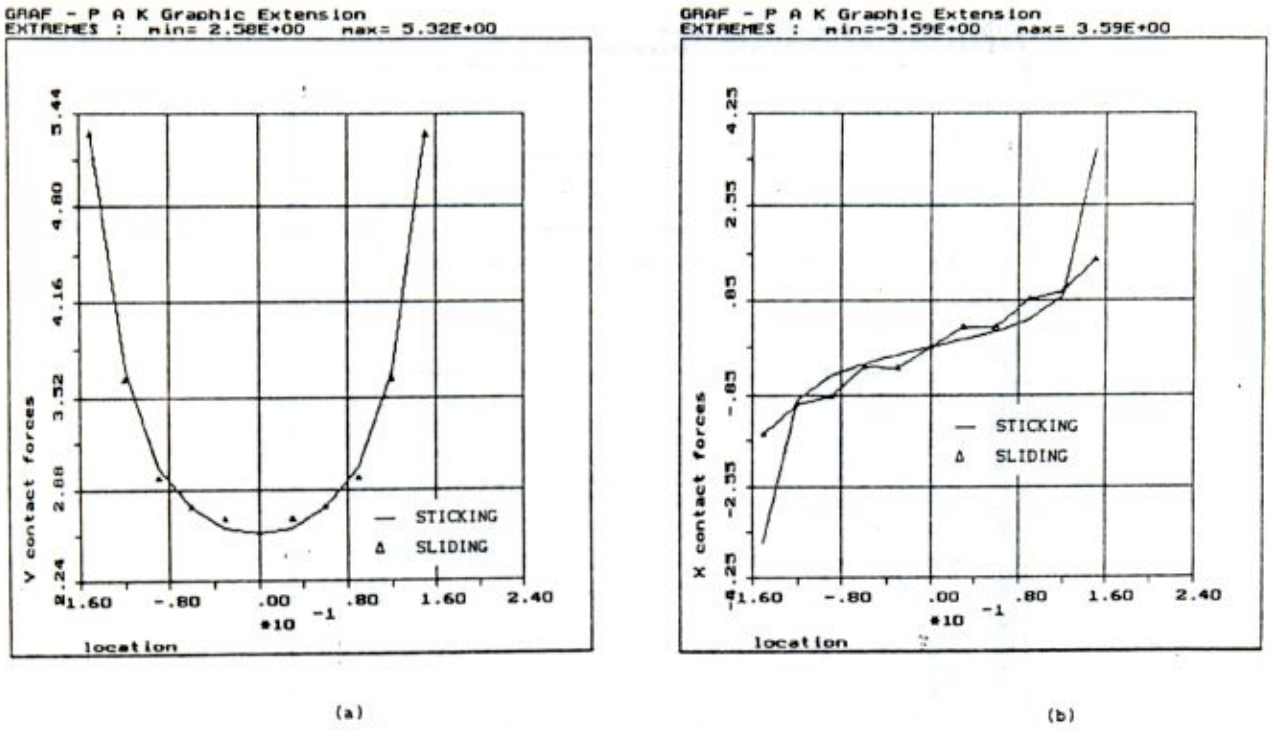

Figure 8. Contact forces distribution
(a) normal distribution
(b) tangential direction

Two cases are analyzed (a) sticking, and (b) sliding with friction coefficient between the foot and soil $\mu = 0.3$. In Fig. 8 we show the field of the mean plastic strain in case of sliding conditions, and in Fig. 9 the normal and tangential force distribution is given. Both figures 8 and 9 correspond to the last step. We have solved the footing problem with different number of steps. In Table 5 are given values of the contact force for selected number of steps. We see that the force values do not differ significantly, illustrating, as in Example 1, high accuracy of the developed algorithm.

Table 5. Final contact force for footing problem

Number of steps	Contact force [kN]
10	35.14
2	33.64
1	31.99

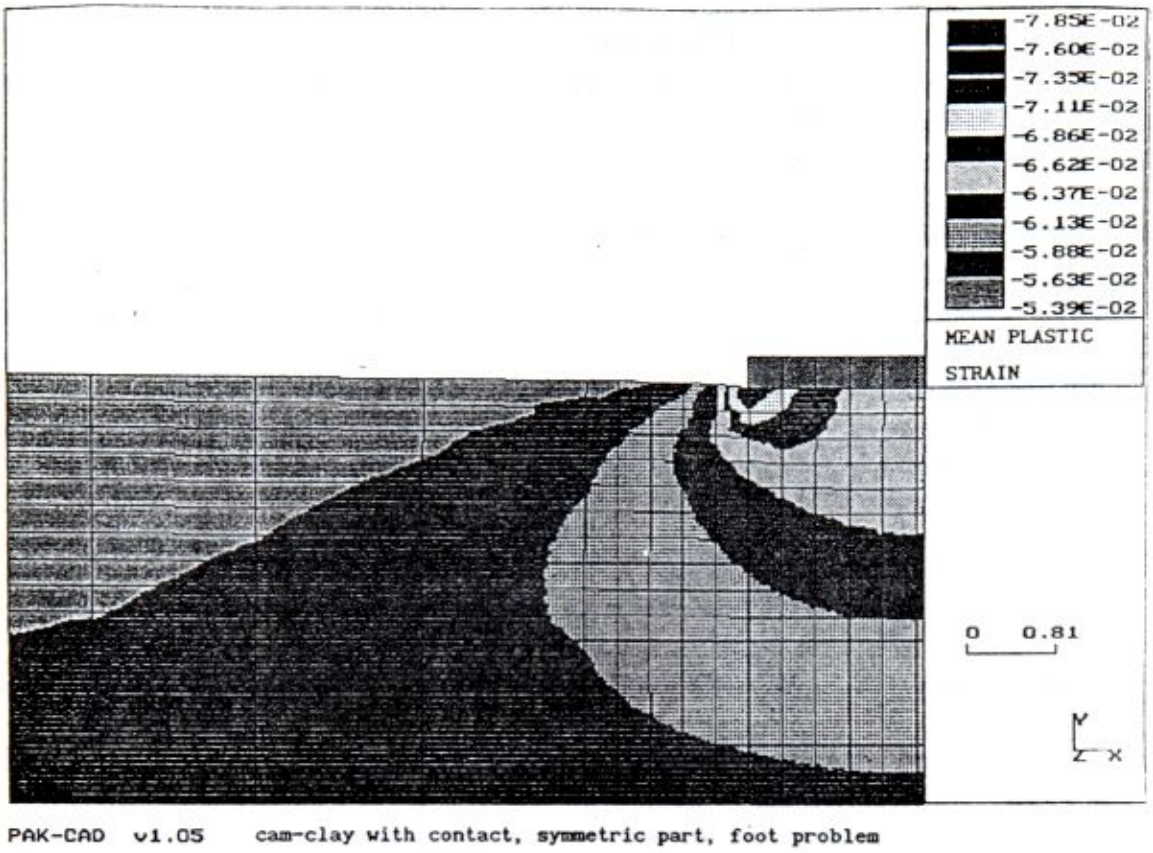

Figure 9.

5. Conclusions

We have presented a complete implicit procedure for stress integration of the modified Cam-clay material model, which includes hardening behavior and the critical stress state conditions. The developed algorithm, representing an application of the governing parameter method (GPM), is computationally efficient since the stress calculation is reduced to solution of one nonlinear equation, with several trials. As it is implicit, the algorithm is accurate, and also it is robust since it is applicable to large strain increments. The tangent elastic-plastic matrix provides high convergence rate in the analysis, as shown in the solved examples. Taking into account the above mentioned characteristics, the presented computational procedure has advantages with respect to others published in literature [6], [7], [14], [15].

The examples illustrate applicability of the algorithm to engineering problems, which, with use of the efficient iterative solution methods and contact algorithm (as in the program PAK [11]), can be successfully employed in practice.

REFERENCES

[1] Kojic, M., *A General Concept of Implicit Integration of Constitutive Relations for Inelastic Material Deformation*, (in Serbian), Center for Scientific Research of Serbian Academy of Sciences and Arts and Univ. of Kragujevac, Kragujevac, (1993).

[2] Desai,C.S. and Siriwardane, N., *Constitutive Laws for Engineering Materials*, Prentice-Hall, Englewood Cliffs, N.J., (1984).

[3] Chen, F.C., *Plasticity in Reinforced Concrete*, McGraw-Hill Book Co., N.Y.. (1982).

[4] *Constitutive Equations in Viscoplasticity*: Computational and Engineering Aspects, The winter annual meeting of ASME, N.Y., (1976).

[5] Krieg, B.D. and Krieg, D.B., *Accuracies of numerical solutions methods for the elastic-perfectly plastic model*, ASME J. Press. Wess. Tech., v.99 (1977), pp. 510–515.

[6] Ortiz, M., and Simo, J.C., *An analysis of new class of intergration algorithms for elastoplastic contitutive relations*, Int. j. numer. methods eng., v. **23** (1986), pp. 353–366.

[7] Simo, J.C., Kennedy, J.G., and Govindjee, S., *Non-smooth multisurface plasticity and viscoplasticity. Loading (unloading) conditions and numerical algorithms*, Int. j. numer. methods eng., v. **26** (1988), pp. 2161–2185.

[8] Kojić, M., and Bathe, K.J., *The effective-stress- function algoithm for thermo-elasto-plasticity and creep*, Int. j. numer. methods eng., v. **24** (1987), pp. 1509–1532.

[9] Kojić, M., and Bathe, K.J., *Thermo-elastic- plastic and creep analysis of shell structures*, Comp. Struct., v. **26** No 1/2, (1987), pp. 135–143.

[10] Kojić, M., *Computational Algorithms in Inelastic Analysis of Solids and Structures*. In preparation.

[11] Kojić, M., Slavković, R., Živković, M., Grujović, N., *PAK-Finite Element Program for Structural Analysis*, Mašinski fakultet, 34000 Kragujevac, Yugoslavia.

[12] Burland, J.B., *The yielding and dilatation of clay*; correspondence, Géotechnique, v. **15**, No. 2, (1965), pp. 211–219.

[13] Roscoe, K.H., and Burland, J.B., *On the generalized stress-strain behavior of wet clay*, in Engineering Plasticity, Eds. J. Heyman and F. A. Leckie, Cambridge Univ. Press, London, (1968), pp. 535–609.

[14] Borja, R., and Lee, S., Cam-clay plasticity, part I: *Implicit integration of elasto-plastic constitutive relations*, Com. Meth. Appl. Mech. Engng, **78** (1990), pp. 49–72.

[15] Borja, R., Cam-clay plasticity, part II: *Implicit integration of constitutive equation based on a nonlinear elastic stress predictor*, Comp. Meth. Appl. Mech. Engng, **88** (1991), pp. 225–240.

[16] Kojić, M., Slavković, R., Grujović, N., Živkovic, M., *A general anisotropic metal plasticity model-model definition and implicit stress integration procedure*, submitted for publication in an international journal.

[17] Kojic, M., Zivkovic, M., and Kojic, A., *Elastic- plastic analysis of orthotropic multilayered beam*, submitted for publication in an international journal.

[18] Kojic, M., Grujovic, N., Kojic, A., *Solution procedure for elastic-plastic orthotropic multilayered pipe deformation under external load and internal pressure*, submitted for publication in an international journal.

[19] Kojic, M., Grujovic, N., Slavkovic, R., and Zivkovic, M., *A general orthotropic von Mises plasticity material model – model definition and implicit stress integration procedure*, submitted for publication in an international journal.

[20] Kojic, M., Slavkovic, R., Grujovic N., and Zivkovic, M., *Implicit stress integration procedure for the generalized cap model in soil plasticity*, submitted for publication in an international journal.

[21] Kojic, M., *Implicit stress integration of the viscoplacity constitutive relations by the governing parameter method (GPM)*, submitted for publication in an international journal.

L'ARGORITHME D'INTÉGRATION IMPLICITE DE LA CONTRAINTE CONCERNANT LE CAM–CLAY (L'ARGILE) MODÈLE MODIFIÉ

L' algorithme d'intégration implicite de la contrainte concernant le Cam-clay (l'argile) modèle du matérial est présenté dans cet article. Le comportement du matérial est représenté par des ellipses avec les caractéristiques de renforcement et la ligne d'état de contrainte critique.

L'algorithme est développé pour l'intégration de contrainte á partir des déformations totales connues (strain-driven problémes) et il est appliqué á l'analyse incrémentale dans la méthode des éléments finis. Le problème d'estimation de la contrainte au bout du pas de charge est réduit á la résolution d'une équation non-linéaire. Ce procédé constitue l'application du paramètre fondamental (GPM) développé dans Réf. [1]. Les régimes de renforcement et d'amolissement sont analysés en détail. La matrice élastique-plastique constitutive est déduite par rapport á l'algorithme d'integration de la contrainte.

La matrice constitutive assure la vitesse quadratique de convergence pour l'analyse incrémentale itérative appliquée dans la méthode des éléments finis.

L'algorithme est illimité, sûr et efficace: il garantit une grande précision ce qui est illustré par la comparaison avec des résultats disponsibles dans la iltterature citée. L'avantage particulier de l'algorithme est son application dans l'analyse des éléments finis á partir de la méthode de déplacement. La méthodologie est intégrée dans un paquet de programme d'application générale basé sur la méthode des éléments finis PAK.

Le probléme caractéristique de charge du sol est résolu en utilisant l'interaction entre la construction et le sol.

ALGORITAM IMPLICITNE INTEGRACIJE NAPONA ZA MODIFIKOVANI CAM–CLAY (GLINA) MATERIJALNI MODEL

U radu je prikazan algoritam implicitne integracije napona za modifikovani Cam-clay (glina) materijalni model. Ponašanje materijala je predstavljeno elipsama sa karakteristikama ojačanja i sa linijom kritičnog stanja.

Algoritam je razvijen za integraciju napona pri poznatim ukupnim deformacijama ("strain-driven" problemi) i primenjen je u inkrementalnoj analizi u metodu konačnih elemenata. Problem određivanja napona na kraju koraka opterećenja svodi se na rešavanje jedne nelinearne jednačine i postupak predstavlja primenu metoda osnovnog parametra (GPM) razvijenog u Ref. [1]. Režimi ojačanja i omekšanja su detaljno analizirani. Izvedena je konstitutivna elasto–plastična matrica saglasna sa algoritmom za integraciju napona.

Konstitutivna matrica obezbeđuje kvadratni koreni stepen (brzinu) konvergencije u inkrementalno–iterativnoj analizi u metodu konačnih elemenata.

Algoritam nema ograničenja u primeni, pouzdan je i efikasan; obezbeđuje veoma dobru tačnost, koja je prikazana kroz poređenje rezultata sa raspoloživim u citiranoj literaturi. Posebna pogodnost je u primeni algoritma kod analize

konačnih elemenata baziranog na metodu pomeranja. Metodologija je ugrađena u programski paket opšte namene baziran na metodu konačnih elemenata PAK.

Rešen je tipičan primer nosivosti tla, uz korišćenje algoritma za rešavanje kontaktnih problema za modeliranje interakcije između konstrukcije i tla.

Miloš Kojić
Faculty of Mechanical Engineering, 34000 Kragujevac, Yugoslavia
Radovan Slavković
Faculty of Mechanical Engineering, 34000 Kragujevac, Yugoslavia
Nenad Grujović
Faculty of Mechanical Engineering, 34000 Kragujevac, Yugoslavia
Mirjana Vukićević
Faculty of Civil Engineering, 11000 Belgrade, Yugoslavia